Self-organized phenomena of pedestrian counter flow in a channel under periodic boundary conditions*

Li Xiang(李 翔)[a)], Duan Xiao-Yin(段晓茵)[a)], and Dong Li-Yun(董力耘)[a)b)†]

[a)] *Shanghai Institute of Applied Mathematics and Mechanics, Shanghai University, Shanghai* 200072, *China*
[b)] *Shanghai Key Laboratory of Mechanics in Energy Engineering, Shanghai* 200072, *China*

(Received 1 March 2012; revised manuscript received 16 April 2012)

In this paper we investigate self-organized phenomena such as lane formation generated by pedestrian counter flow in a channel. The lattice gas model is extended to take the effect of walkers in the opposite direction into account simultaneously when they are in the view field of a walker, i.e., walkers tend to follow the leaders in the same direction and avoid conflicts with those walking towards them. The improved model is then used to mimic pedestrian counter flow in a channel under periodic boundary conditions. Numerical simulations show that lane formation is well reproduced, and this process is rather rapid which coincides with real pedestrian traffic. The average velocity and critical density are found to increase to some degree with the consideration of view field.

Keywords: counter flow, lattice gas model, view field, lane formation

PACS: 89.40.Bb, 02.50.Cw, 05.50.+q **DOI:** 10.1088/1674-1056/21/10/108901

1. Introduction

Recently, more and more attention has been paid to pedestrian traffic, especially, self-organized phenomena and collective behaviour in various situations.[1−6] The simplest and most widely-studied case is the pedestrian counterflow in a channel, and the emergent lane formation has been observed experimentally and investigated numerically.[7−20] In contrast to macroscopic description (e.g. the hydrodynamic model[2]), microscopic models can better characterize detailed interactions among pedestrians, e.g., the social force model.[3] The social force model is actually a kind of molecular dynamic model where both space and time are continuous. Pedestrians are treated as Newton-like particles driven by attractive and repulsive forces. It is shown that such a model can reproduce most of the interesting phenomena of pedestrian flow in reality.

Hereafter, discrete microscopic models such as cellular automaton models[4,5] and lattice gas model[7] are proposed as well. Helbing *et al.*[6] mentioned that lane formation is hard to describe by cellular automata. However, Burstedde *et al.*[4] suggested a cellular automaton model to depict collective phenomena, e.g. lane formation by introducing so-called floor fields. The static floor field transfers global information to each pedestrian which does not evolve with time. The dynamic floor field is to model the attractive interaction among pedestrians which is the key to reproducing lane formation. On the other hand, the lattice gas (LG) model has exhibited phase transition from the freely moving phase to the jamming phase. In this model the random sequential updating rule is adopted and therefore it is easy to deal with conflicts among pedestrians. Hereafter, more elaborate factors of human behaviour were introduced into this model in order to obtain a better description of pedestrian traffic.[8−20] However, most of these modified models failed to reproduce the lane formation with common sense. The first successful attempt was the introduction of a view field by Tajima *et al.*[8] which could be regarded as a kind of long-range interaction. They studied the effect of pedestrians walking in the same and opposite directions, respectively. They have shown that both mechanisms lead to lane formation but are quite different. Recently, Ma *et al.*[9] adopted a multi-grid model to reproduce such a pattern formation as well. The multi-grid model is in fact regarded

*Project partially supported by the National Basic Research Program of China (Grant No. 2012CB725404), the National Natural Science Foundation of China (Grant Nos. 10972135 and 11172164), the Innovation Program of Shanghai Municipal Education Commission, China (Grant No. 11YZ12), the Shanghai Program for Innovative Research Team in Universities, and the Program for Changjiang Scholars and Innovative Research Team in Universities, China (Grant No. IRT0844).

†Corresponding author. E-mail: dly@shu.edu.cn

© 2012 Chinese Physical Society and IOP Publishing Ltd

as a refined lattice gas model in which the size of a site is smaller and a pedestrian can occupy more than one site. Only the effect of pedestrians in opposite directions in the view field has been taken into account. Both studied the pedestrian counterflow in a channel under open boundary conditions. By contrast, the rule suggested by Ma *et al.*[9] is simpler than that by Tajima *et al.*,[8] but the calculations proposed by Ma *et al.* are more than those proposed by Tajima *et al.*. Obviously, a model with simple rules and less computation is preferred. It is also believed that pedestrians in the same and opposite directions in the view field simultaneously influence the behaviour of a pedestrian. Furthermore, the self-organized behaviour of pedestrians is rather fast, e.g. lane formation in the pedestrian crosswalk, but such a feature has not attracted sufficient attention so far.

In this paper, an extended lattice gas model is used to investigate the pedestrian counter flow in a channel under periodic boundary conditions. The rest of the present paper is organized as follows. In Section 2, the lattice gas model is improved to take the effect of pedestrians in the same and opposite directions in the view field of each pedestrian into account simultaneously. Numerical simulations are carried out and discussions about lane formation and fundamental diagrams with different parameters are given in Section 3. Conclusions and suggestions for further research are presented in Section 4.

2. Model

The extended lattice-gas model is defined as the square lattice of $L \times W$ sites where L (W) is the length (width) of the channel. Figure 1 shows the schematic illustration of the pedestrian counter flow in a channel. There are two kinds of pedestrians in the system. Each walker moves to the preferential direction with no back step, i.e., from left to right or from right to left. The right (left) walker going to the right (left) is indicated by the open (full) circle. Each site can be occupied by only a single walker. The top and bottom sides are a solid wall and therefore walkers never go out through the wall. The boundary condition in the horizontal direction is periodic. When a right (left) walker leaves the system from the right (left) boundary, he enters into the system from the left (right) boundary immediately. The total density ρ is defined as the number of all walkers divided by the system size. The density of left (right) walkers $\rho_{\rm l}(\rho_{\rm r})$ is determined by calculating the fraction of the left walker f, i.e., we have $\rho_{\rm l} = \rho f$ and $\rho_{\rm r} = \rho(1-f)$.

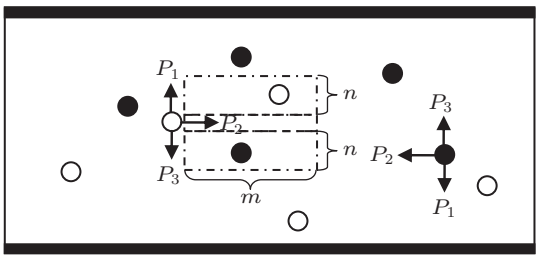


Fig. 1. Schematic illustration of the pedestrian counter flow in a channel under periodic boundary conditions.

Each walker has a preferential direction and he can shift left, move forward or shift right to his nearest neighbours in a single time step according to the corresponding probabilities (see Fig. 1). Therefore, the state of his possible target site is denoted by an array of three components, 0 means empty and 1 occupied, e.g. (0,1,0) means that the left and right side are empty and the site in front is occupied. Table 1 shows the transition probabilities of a walker determined by the states of his nearest-neighbour sites, where D indicates the strength of the drift. It should be noted that such a description of this model is more general and convenient to use in other cases, e.g., the preferential direction is diagonal.

Table 1. Transition probabilities to the nearest-neighbour sites are given by p_1 (left), p_2 (front), and p_3 (right).

State	(0,0,0)	(0,0,1)	(0,1,0)	(0,1,1)	(1,0,0)	(1,0,1)	(1,1,0)	(1,1,1)
p_1	$(1-D)/3$	$(1-D)/2$	$1/2$	1	0	0	0	0
p_2	$D+(1-D)/3$	$D+(1-D)/2$	0	0	$D+(1-D)/2$	1	0	0
p_3	$(1-D)/3$	0	$1/2$	0	$(1-D)/2$	0	1	0

In fact, a walker interacts not only with his nearest-neighbour walkers but also with others in his view field. As is well known, a walker tends to follow the leader in the same direction and keeps away from those in the opposite direction. In this paper, the view field of a walker is represented by a rectangle area, which is divided into three parts, i.e., front left, front, and front right. Both front left and right parts

have the same size of $m \times n$ where m (n) is the length (width) of the corresponding part. The front part has a size of $m\times1$, thus the total size of the view field is $m\times(2n+1)$. The structure of the view field is similar to that in Tajima *et al.*,[8] but different from that in Ma *et al.*[9] A walker will adjust the transition probability according to the number of other walkers in the same or opposite direction.

The movement of each walker is determined by the following rules.

(i) Calculate the transition probabilities p_1, p_2, and p_3 of each walker according to the states of his nearest-neighbour sites as shown in Table 1;

(ii) Count the number of walkers in the same (opposite) direction in the front left, front, and front right of view field respectively, which are denoted by $T_1(S_1)$, $T_2(S_2)$, and $T_3(S_3)$ respectively;

(iii) Calculate the final transition probabilities P_1, P_2, and P_3 according to the following formula:

$$P_i = \frac{p_i(T_i+1)/(S_i+1)}{\sum_{j=1}^{3} p_j(T_j+1)/(S_j+1)}, \quad i = 1, 2, 3.$$

The formula indicates that the transition probabilities are proportional to the number of walkers in the same direction but inversely proportional to the number of walkers in the opposite direction. When a walker aims to enter one of target sites, his intention becomes stronger, and the more walkers there are in the same direction, on the contrary, his intention becomes weaker, and the more walkers there are in the opposite direction. It is easy to find that we need only to calculate the final transition probability in cases 1, 2, 3, and 5 in Table 1. Finally, the states of all walkers are updated sequentially in a random order.[7]

3. Simulation and discussion

The simulation of pedestrian counterflow in a channel is performed under periodic boundary conditions. The size of a site corresponds to approximately 0.4 m×0.4 m, which is the typical space occupied by a person in a dense crowd.[4] Usually the average velocity of a pedestrian is about 1.2 m/s for a walker. Thus, each time step corresponds to 1/3 s. Initially, walkers with a given density are distributed randomly in the system. The average velocity in each time step is defined as the number of walkers moving to their preferential direction divided by the total number of walkers existing in the system. The average flux is the product of total density and average velocity. Each run of the simulation takes 10^3 time steps. The final results are the average of 50 runs of the simulation.

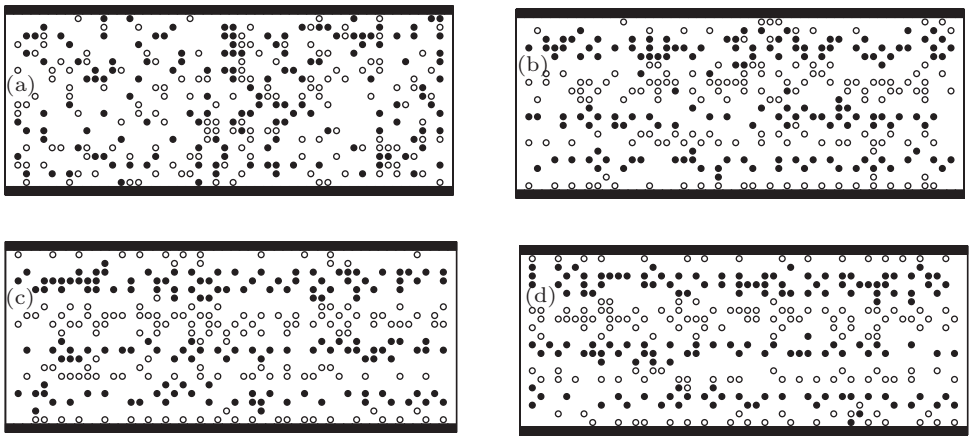


Fig. 2. Simulated scenarios at different time steps, where $W = 20$, $L = 50$, $D = 0.6$, $m = 20$, $n = 3$, $f = 0.5$, $\rho = 0.3$, $t = 0$ (a), 15 (b), 30 (c), and 60 (d).

First we investigate typical flow patterns generated by the present model. Figure 2 shows the simulated scenarios at different time steps. Initially walkers are distributed randomly in the channel (See Fig. 2(a)). It is found that eight lanes are formed quickly and the system reaches its steady state quickly. Without the view field, walkers have to interact with each other directly when they get close. As a result, they have less chance to adjust their paths in advance and then small local congestions may occur occasionally. Under certain conditions, these small congestions may spread and finally form complete congestions. With the consideration of walkers in the same and opposite direction together in the view field, a

long-range interaction is introduced and walkers have the chance to avoid conflicts with those walking in the opposite direction in advance and tend to follow the leader in the same direction. To this end, lanes of uniform direction are segregated from pedestrian counter flow.

Figure 3 shows the average densities along the channel for the left (Fig. 3(a)) and right (Fig. 3(b)) walkers in a larger system size. It is found that five lanes are formed by left walkers and five lanes are formed by right walkers (note that there is a small lane near the top wall in Fig. 3(b)). In general, the number of lanes increases with the increase of the width of channel. But for a channel with a given width, the number of lanes formed is dynamic in various simulations, which is not constant as pointed out by Helbing[1] but similar to that in Ma *et al.*[9] Furthermore, the number of lanes in two directions are not necessarily equal. One can see that the system reaches its steady state in a short time (about 20 seconds in Fig. 3). It should be noted that it will take a longer time to reach the steady state under open boundary conditions. Even so, the effect of walkers from both directions is expected to be stronger than that of walkers only in the same or opposite direction. As shown in Fig. 4, the number of lanes decreases with the increase of the width of the view field for a given

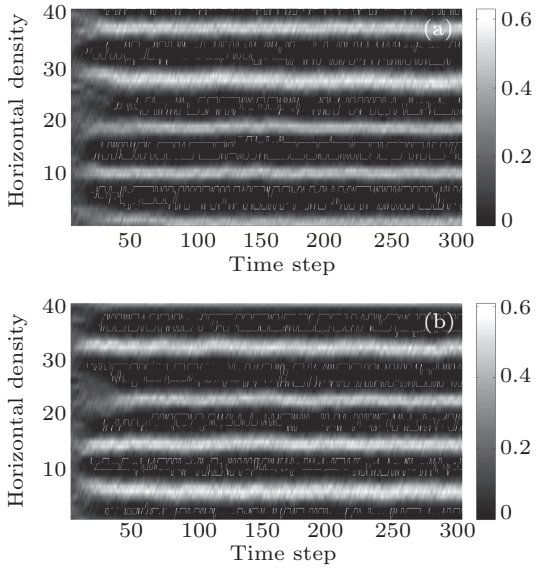


Fig. 3. Density profile evolutions at $W = 40$, $L = 100$, $D = 0.6$, $\rho = 0.3$, $f = 0.5$, $m = 20$, and $n = 3$, where panel (a) shows the left walkers and panel (b) exhibits the right walkers.

parameter set. To obtain a realistic result, we choose the following parameters, i.e., $m = 20$ and $n = 3$ for most cases.

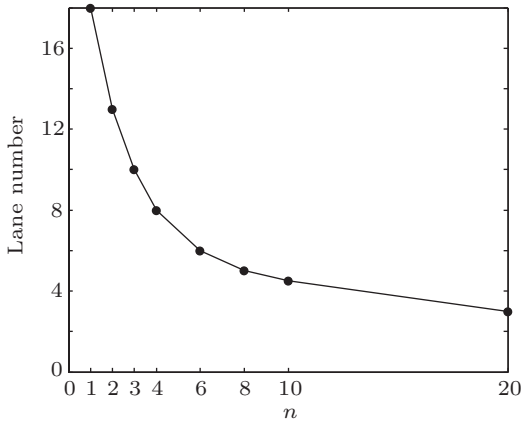


Fig. 4. The relationship between the number of lanes and the width of the view field at $L = 100$, $W = 40$, $D = 0.6$, $m = 20$, and $f = 0.5$.

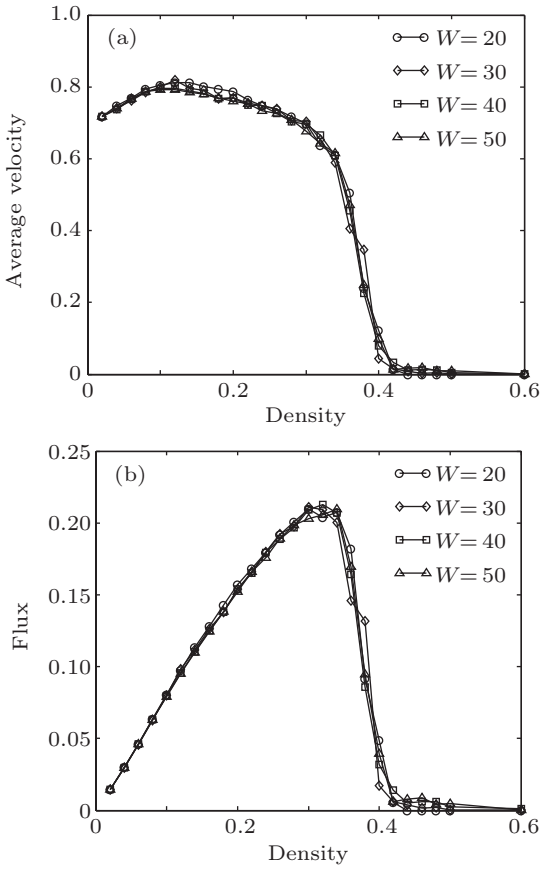


Fig. 5. (a) Plots of average velocity against total density at $W = 20$, 30, 40, and 50, where $L = 50$, $D = 0.6$, $m = 20$, $n = 3$, and $f = 0.5$, and (b) plots of the flux against the total density at the same data as those in panel (a).

Then we investigate the effect of system size on the relationship between average velocity and total density. As shown in Fig. 5, one can see that the trends of the curves are almost the same although more lanes form in wider channels, which means that

the average velocity of walkers is nearly independent of channel width for a given view field. So we choose $W = 20$ in the following simulations. It is found that the average velocity first increases, then decreases and finally vanishes. This result will be discussed later in more detail.

As mentioned in Section 2, the view field indeed introduces a long-range interaction rather than an immediate interaction in the original LG model. Therefore, it is expected that the size of the view field has a vital influence on the collective behaviour of walkers. Figures 6 and 7 show the simulation results for different lengths and widths of the view field, respectively. The result of the LG model is also presented for comparison. From Fig. 6, one can see that the average velocity and the flux increase with the increase of the length of the view field as well as the critical density. In general, the average velocity and the flux are larger than those in the LG model before phase transition except $m = 5$. The critical density is always larger than that in the LG model, but it does not have a significant difference for different lengths of the view field. As shown in Fig. 7, the average velocity and the flux increase with the length of the view field as well as the critical density, which are always larger than those in the LG model. But the average velocity and the flux do not have significant differences for different widths of the view field before phase transition. In general, the total effect of the view field is the increase of the average velocity and the flux as well as the critical density compared with that in the LG model. Therefore, the introduction of the view field indeed enhances the efficiency of walking.

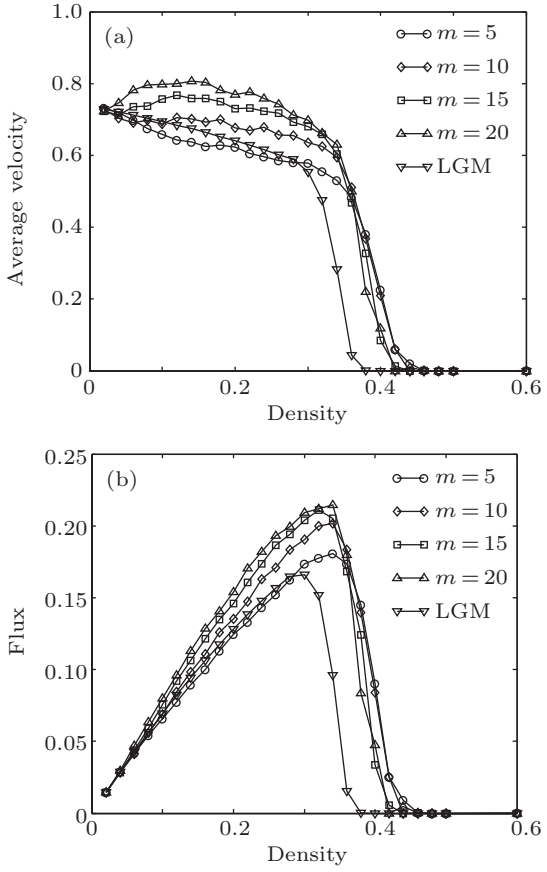


Fig. 6. (a) Plots of average velocity against total density for $m = 5$, 10, 15, 20, and LGM at $L = 50$, $W = 20$, $n = 3$, $D = 0.6$, and $f = 0.5$, and (b) plots of flux against total density for the same data as those in panel (a).

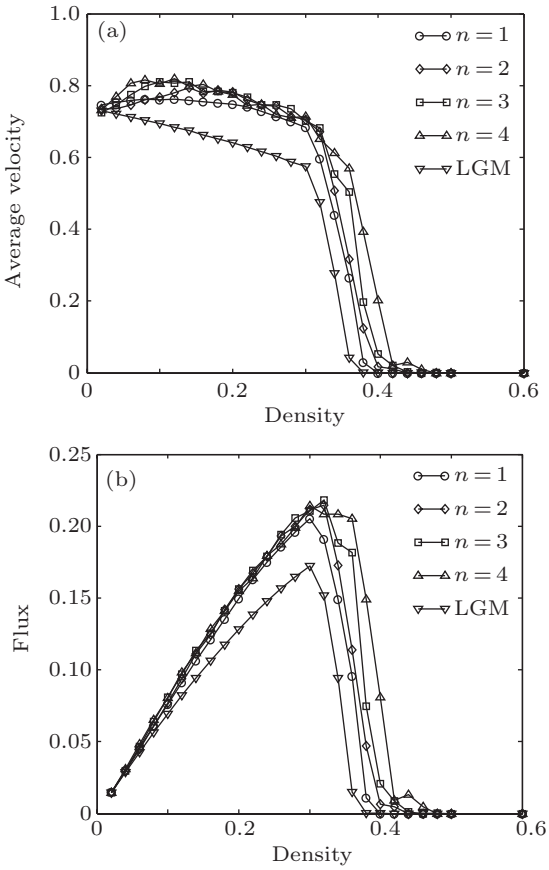


Fig. 7. (a) Plots of average velocity against total density for $n = 1$, 2, 3, 4, and LGM at $L = 50$, $W = 20$, $m = 20$, $D = 0.6$, and $f = 0.5$, and (b) plots of the flux against total density for the same data as those in panel (a).

Furthermore, we investigate the effect of the fraction of left walkers on the counter flow in the channel. As shown in Fig. 8(a), there is a negligible difference in the very low density regime since few walkers exist in the system and the interactions among them are weak. With density increasing, the largest average velocity and flux appear in the symmetric case ($f = 0.5$). However, the largest critical density appears in the most asymmetric case ($f = 0.1$). The possible reasons for this are as follows: when f is rather small, the number of walkers on the right is much larger than that of

walkers on the left. The attraction among walkers on the right becomes dominant and the repulsion from walkers on the left becomes rather weak. As a consequence, a walker on the right is usually blocked by other walkers on the right and the average velocity reduces correspondingly. On the contrary, it is not easy to form global congestion, owing to a lack of walkers from the opposite direction. In the symmetric case, the average velocity and the flux reach their maxima due to self-organized lane formation which makes the counter flow more efficient before phase transition occurs.

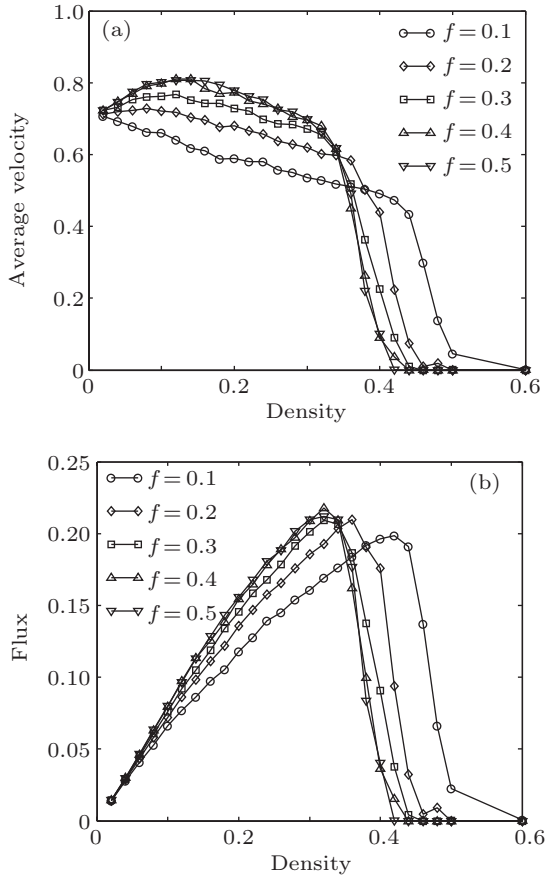


Fig. 8. (a) Plots of the average velocity against the total density for $f = 0.1$, 0.2, 0.3, 0.4, and 0.5 at $L = 50$, $W = 20$, $m = 20$, $n = 3$, and $D = 0.6$, and (b) plots of the flux against total density for the same data as those in panel (a).

Finally, we study the effect of the strength of drift on the collective behaviour of walkers. It is found that the average velocity and flux increase with D in the freely moving phase which is shown in Fig. 9. As mentioned before, the average velocity first increases in the low density range, then decreases slowly in the medium density range, and finally vanishes in the high density range. Similar results have been reported in Ref. [9]. Moreover, one can see that the low density range reduces with D. When D becomes larger, such an effect becomes less noticeable. On the other hand, the critical density becomes lower as D increases. This can be explained by the effect of 'faster-is-slower'.[1,21] In the high density regime, walking slowly is better than walking as quickly as possible.

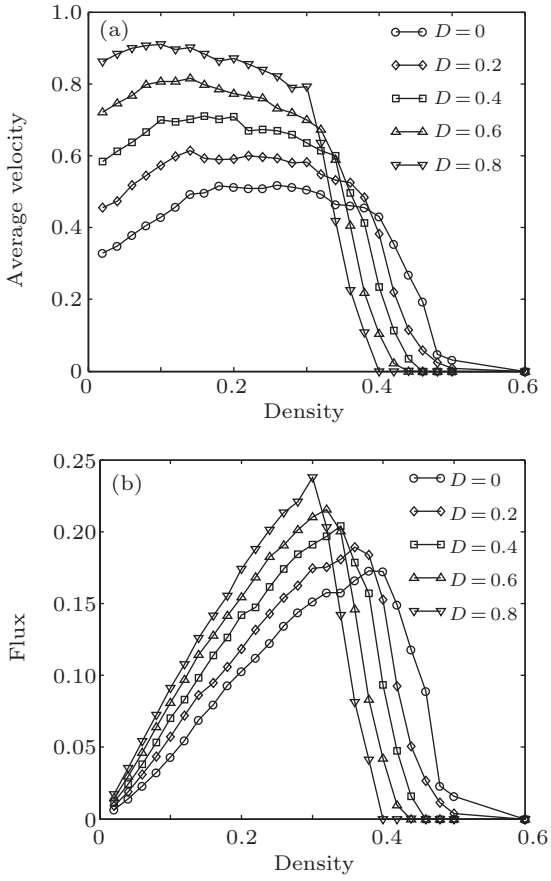


Fig. 9. (a) Plots of average velocity against total density for $D = 0$, 0.2, 0.4, 0.6, and 0.8 at $L = 50$, $W = 20$, $m = 20$, $n = 3$, and $f = 0.5$. Walkers move forward with an average velocity of $D + (1 - D)/3$ at very low densities. (b) Plots of flux against total density for the same data as those in panel (a).

In the LG model, one may notice that the average velocity decreases with density increasing monotonically (see Figs. 6(a) and 7(a)). In this model, each walker has an equal probability to move forward, left or right in the case of $D = 0$ and he behaves randomly. When D increases, the walker has a stronger intention to move toward the preferential direction. In a very low density, walkers move freely with negligible conflicts, and as expected, the average velocity reaches its maximum. However, with density increasing, conflicts among walkers in opposite directions becomes more serious since they are blocked by others frequently, as they have to brake or shift and thus the efficiency of walking is reduced noticeably. This is the reason why

the the average velocity is a decreasing function of density in the LG model.

As for the present model, in contrast, walkers in opposite directions separate into lanes of uniform walking direction below the critical density, which reduces the number of conflicts with opposing walkers significantly, i.e., the interaction frequency and number of necessary braking or avoidance manoeuvres is reduced.[21] The attraction of walkers in the same direction and the repulsion of walkers in the opposite direction really strengthens the intention of walkers moving in a preferential direction, i.e., P_2 increases as the number of walkers increases. Therefore, the average velocity in the preferential direction is enhanced, especially in the low density range (see Figs. 5(a)–8(a)). As pointed out by Helbing *et al.*[21] this phenomenon can be viewed as an example of optimal self-organization. For higher densities, walkers are blocked by their leaders even they have the same direction. Although with the help of the view field, the average velocity decreases gradually. This is similar to the case of multilane vehicular traffic. Therefore, the freely moving phase is characterized by lane formation which is different from that in the LG model. Helbing *et al.*[21] have performed several experiments for a corridor with bottlenecks to compare the effects of pedestrian counterflows and unidirectional flows. They also found that counterflows are significantly more efficient than unidirectional flows.[21] Above the critical density, lane formation becomes impossible since small local congestions occur and cannot dissolve promptly, which eventually leads to complete congestion. This process is quantitatively similar to that in the LG model but the underlying mechanism may be qualitatively distinct.

4. Summary

In this paper, we proposed an extended lattice gas model with consideration of the effect of walkers in the same and opposite directions, i.e., a walker tends to follow the leader in the same direction and avoid collision with those from the opposite direction. Then we used this model to investigate dynamical collective behaviours of pedestrian counterflow in a channel. More attention was paid to lane formation, especially the efficiency of reproducing such a collective behaviour. In the symmetric case of $f = 0.5$, it is found that the effect of walkers in both the same and opposite directions in the view field strengthens the intention of the walker to move to their preferential directions and pedestrian counter flow is separated into lanes of uniform walking direction effectively. The conflicts among walkers are reduced significantly and therefore the efficiency of walking is enhanced due to lane formation. Both the average velocity and the flux increase to some degree as well as the critical density in comparison with those from the LG model. This can be viewed as an example of optimal self-organization. It turns out that this model provides a more realistic description of pedestrian flow and can be further applied to other cases.

References

[1] Helbing D 2001 *Rev. Mod. Phys.* **73** 1067

[2] Hughes R L 2002 *Transp. Res.* B **36** 507

[3] Helbing D and Molnàr P 1995 *Phys. Rev.* E **51** 4282

[4] Burstedde C, Klauck K, Schadschneider A and Zittartz J 2001 *Physica* A **295** 507

[5] Kirchner A and Schadschneider A 2002 *Physica* A **312** 260

[6] Helbing D, Farkas I J, Molnàr P and Vicsek T 2002 *Pedestrian and Evacuation Dynamics* 21

[7] Muramatsu M, Irie T and Nagatani T 1999 *Physica* A **267** 487

[8] Tajima Y, Takimoto K and Nagatani T 2002 *Physica* A **313** 709

[9] Ma J, Song W G and Liao G X 2010 *Chin. Phys.* B **19** 128901

[10] Ma J, Song W G, Zhang J, Lo S M and Liao G X 2010 *Physica* A **389** 2101

[11] Peng Y C and Chou C I 2011 *Comput. Phys. Commun.* **182** 205

[12] Kuang H, Li X L, Wei Y F, Song T and Dai S Q 2010 *Chin. Phys.* B **19** 070517

[13] Kuang H, Song T, Dai S Q and Li X L 2009 *Int. J. Mod. Phys.* C **20** 1945

[14] Kuang H, Li X L, Song T and Dai S Q 2008 *Phys. Rev.* E **78** 066117

[15] Li J, Yang L H and Zhao D L 2005 *Physica* A **354** 619

[16] Weng W G, Pan L L, Shen S F and Yuan H Y 2007 *Physica* A **374** 821

[17] Weng W G, Shen S F, Yuan H Y and Fan W C 2007 *Physica* A **375** 668

[18] Hao Q Y, Hu M B, Cheng X Q, Song W G, Jiang R and Wu Q S 2010 *Phys. Rev.* E **82** 026113

[19] Yue H, Guan H Z, Zhang J and Shao C F 2010 *Physica* A **389** 527

[20] Zhou J W, Chen X L, Zhou J H, Tan H L, Kong L J and Liu M R 2009 *Acta Phys. Sin.* **58** 2281 (in Chinese)

[21] Helbing D, Buzna L, Johansson A and Werner T 2005 *Transport. Sci.* **39** 1